JOC The Journal of Organic Chemistry

Article

pubs.acs.org/joc

Probing the Role of Glycol Chain Lengths in π-Donor−Acceptor [2]Pseudorotaxanes Based on Monopyrrolo-Tetrathiafulvalene and Cyclobis(paraquat-*p*-phenylene)

Rikke Kristensen, Sissel S. Andersen, Gunnar Olsen, and Jan O. Jeppesen*

Department of Physics, Chemistry, and Pharmacy, University of Southern Denmark, Campusvej 55, DK-5230 Odense M, Denmark

Supporting Information

ABSTRACT: We have investigated and quantified the role that the glycol chain length has on the strength of the noncovalent bonding interactions taking place between cyclobis(paraquat-*p*-phenylene) ($CBPQT^{4+}$) and five different monopyrrolo-tetrathiafulvalene (MPTTF) derivatives that only differ in the length of the *N*-substituted glycol chain. The MPTTF derivatives were used to form [2]pseudorotaxanes by mixing them with $CBPQT^{4+}$. The binding constants (K_a) associated with the complexation process leading to the formation of the [2]pseudorotaxanes were obtained using the UV−vis−NIR dilution method and the [2]pseudorotaxanes were characterized structurally using ^{1}H NMR spectroscopy. These experimental investigations clearly indicate that the glycol chains provide additional stability to the [2]pseudorotaxanes findings that were further supported by density functional theory (DFT) studies. The DFT calculated superstructure of the [2]pseudorotaxane **3**⊂$CBPQT^{4+}$ reveal that [C−H···O] hydrogen bonding interactions between the acidic *α-H* protons in $CBPQT^{4+}$ and the oxygen atoms present in the glycol chain can take place on the exterior of the [2]pseudorotaxane. However, the length of the glycol chain is of paramount importance and the present studies show that the first and second oxygen atom in the [2]pseudorotaxanes **2**−**5**⊂$CBPQT^{4+}$ are engaged in [C−H···O] hydrogen bonding interactions with $CBPQT^{4+}$, whereas the third and fourth oxygen atoms are not.

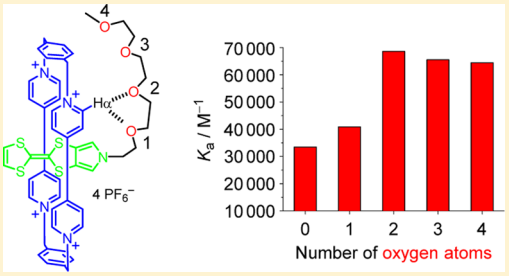

INTRODUCTION

Host−guest complexes constitute an important part of supramolecular chemistry[1] and the noncovalent interactions[2] present in these supramolecular systems have been used as a guiding tool for the synthetic chemist to design and create interlocked compounds,[3] such as catenanes[4] and rotaxanes.[5] Special attention[6] has been paid to catenanes and rotaxanes incorporating the tetracationic π-electron accepting macrocycle cyclobis(paraquat-*p*-phenylene)[7] ($CBPQT^{4+}$, Figure 1) which gives rise to strong charge-transfer (CT) interactions[8] with complementary π-donor guest molecules, such as dioxynaphthalene (DNP),[7c,9] hydroquinone (HQ),[10] and tetrathiafulvalene[11] (TTF). In most bistable [2]rotaxanes based on TTF and $CBPQT^{4+}$, glycol chains have been incorporated into the backbone of the dumbbell to connect the primary and secondary stations. The population ratio of the two translational isomers is reflected in their relative free energies as determined primarily by the strength of noncovalent interactions surrounding the two stations.[12] Control over the reversible linear motion of the $CBPQT^{4+}$ ring component between the stations can be achieved by oxidizing and reducing the TTF unit. It has been concluded[11b,13] that the π-electron-donating ability of the TTF derivatives largely dictates the strength (ΔG° = −3.1 to −6.7 kcal mol^{-1}, in MeCN at 303/298 K[8a,11b]) of their binding to $CBPQT^{4+}$. Thus, the stronger π-electron donors form more stable host−guest complexes with $CBPQT^{4+}$. However, in a more recent study,[13] it was found that triethylene glycol (TEG) chains can assist the complexation process between monopyrrolo-TTF (MPTTF)[14] derivatives and $CBPQT^{4+}$ by 0.3 kcal mol^{-1} on account of its capacity to participate in [C−H···O] hydrogen bonding interactions with some of the *α-H* protons in the bipyridinium units of $CBPQT^{4+}$. Most recently,[15] it has been reported that increasing

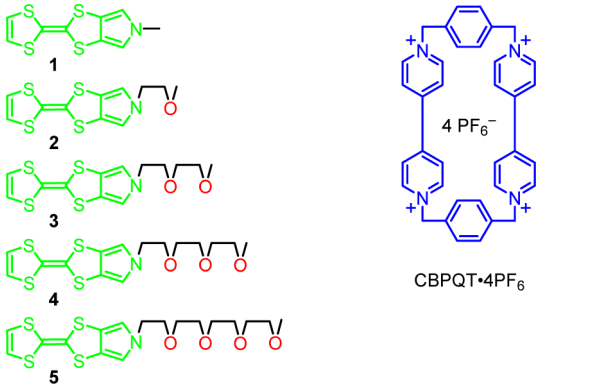

Figure 1. Molecular formulas of the different MPTTF derivatives **1**−**5** and $CBPQT{\cdot}4PF_6$ investigated in the present work.

Received: October 10, 2016
Published: December 27, 2016

DOI: 10.1021/acs.joc.6b02466
J. Org. Chem. 2017, 82, 1371−1379

the station-to-station distance by changing the length of the glycol chains in a homologous series of bistable TTF-rotaxanes had a significant impact on the speed of the linear movement of CBPQT^{4+} between the stations. Despite their importance, there are still only a very few studies,[9,10,16] and to the best of our knowledge none on TTF derivatives, dedicated to elucidate the role of changing the number of ethyleneoxy units present in the glycol chains on the tertiary (3°) superstructure[17] in π-donor−acceptor [2]pseudorotaxanes. In this work, we present the synthesis and investigation of a homologous series of [2]pseudorotaxanes based on the MPTTF derivatives **1**−**5** (Figure 1) and CBPQT^{4+}. This design renders it possible to investigate and quantify the role that the glycol chain length has on the strength of the noncovalent bonding interactions taking place in [2]catenanes and [2]rotaxanes.

RESULTS AND DISCUSSION

As it transpires from Figure 1, the MPTTF derivatives investigated in the present work only differ in the length of the *N*-substituted glycol chain, which is extended by one ethyleneoxy unit across the five MPTTF derivatives **1**−**5**.

Synthesis. The synthesis of compounds **1**−**5** was carried out as illustrated in Scheme 1. Deprotonation of the pyrrole N−H proton in the MPTTF derivative[11] **6** using NaH in DMF followed by *N*-alkylation with the alkylating reagents[18] **7**−**11** gave the MPTTF derivatives **1**−**5** in 82−97% yields.

Scheme 1. Synthesis of the MPTTF Derivatives 1−5

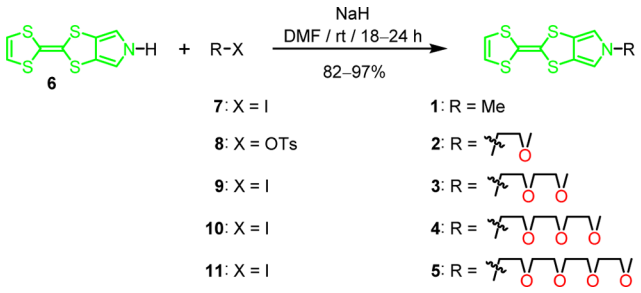

Absorption Spectroscopic Investigations of the Complexation between 1−5 and CBPQT^{4+}. Initial evidence for the formation of the [2]pseudorotaxanes **1**−**5**⊂CBPQT^{4+} came from absorption spectroscopy. Mixing the yellow MPTTF derivatives **1**−**5** with equimolar proportions of the colorless CBPQT^{4+} in MeCN immediately resulted in the formation (Scheme 2) of the [2]pseudorotaxanes **1**−**5**⊂CBPQT^{4+} as evidenced by the spontaneous production of green colored solutions. The UV−vis−NIR absorption spectra (Supporting Information) recorded at 298 K in MeCN of these solutions showed broad CT bands in the 850−880 nm region, an observation which is consistent[11d,19] with the formation of superstructures containing an MPTTF unit inside the cavity of CBPQT^{4+}.

Electrochemistry of the MPTTF Derivatives 1−5. Attachment of electron-donating or electron-withdrawing substituents to the MPTTF unit has a significant impact on the donor strength[14,20] and consequently also on its binding to CBPQT^{4+} (*vide supra*). To ensure that the π-electron donor strength of the MPTTF derivatives **1**−**5** is not affected by the different lengths of the *N*-substituted glycol chains, the first ($E_{1/2}{}^{1}$) and second ($E_{1/2}{}^{2}$) redox potentials were determined using cyclic voltammetry (CV). The cyclic voltammograms (CVs) of **1**−**5** were all measured in MeCN at 298 K and the CVs showed (Table 1 and Supporting Information) as expected two reversible redox waves associated with the two oxidation processes of the MPTTF unit (i.e., MPTTF → MPTTF$^{\bullet+}$ and MPTTF$^{\bullet+}$ → MPTTF^{2+}).[13]

Table 1. First ($E_{1/2}{}^{1}$) and Second ($E_{1/2}{}^{2}$) Redox Potentials for the MPTTF Derivatives 1−5 Obtained by Cyclic Voltammetry[a] (CV) at 298 K in MeCN

compound	$E_{1/2}{}^{1}$[b,c] (V)	$E_{1/2}{}^{2}$[b,c] (V)
1	+0.030	+0.400
2	+0.025	+0.415
3	+0.020	+0.415
4	+0.020	+0.415
5	+0.020	+0.415

[a]CV measurements were carried out in nitrogen-purged MeCN solutions (1.0 mM) with tetrabutylammonium hexafluorophosphate ($TBAPF_6$) as supporting electrolyte (0.1 M), a glassy carbon electrode as working electrode, and at a scan rate of 100 mV s^{-1}. [b]Potential values in V vs Ag/$AgNO_3$. [c]The estimated errors on the $E_{1/2}{}^{1}$ and $E_{1/2}{}^{2}$ values are ±5 mV.

^{1}H NMR Investigations of the Complexation between 1−5 and CBPQT^{4+}. While absorption spectroscopy qualitatively indicate that the MPTTF unit is located inside the cavity of CBPQT^{4+}, ^{1}H NMR spectroscopy can be used as a more quantitative tool for monitoring how the glycol chains present in the MPTTF derivatives **1**−**5** influence the 3° superstructure in the [2]pseudorotaxanes **1**−**5**⊂CBPQT^{4+} and to give fine, as well as gross, structural information.

Support for the observation that the MPTTF unit is located inside CBPQT^{4+} and for the notion that glycol chains influence

Scheme 2. Complexation of the MPTTF Derivatives 1−5 by CBPQT^{4+}

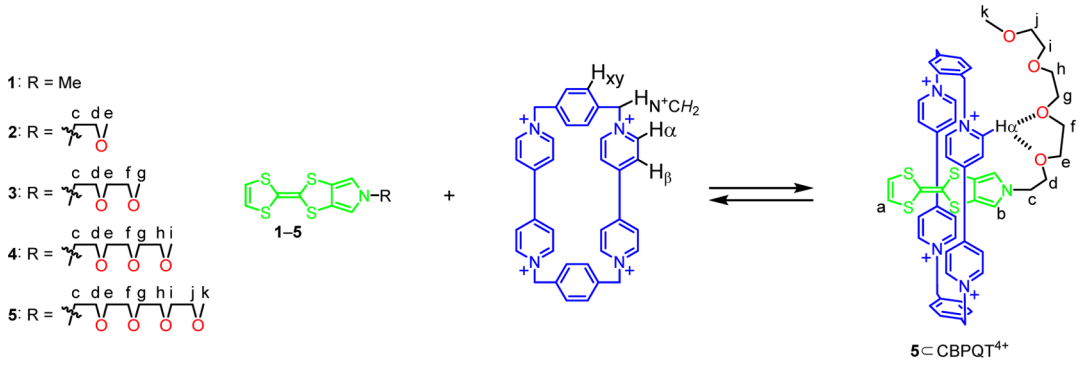

DOI: 10.1021/acs.joc.6b02466
J. Org. Chem. 2017, 82, 1371−1379

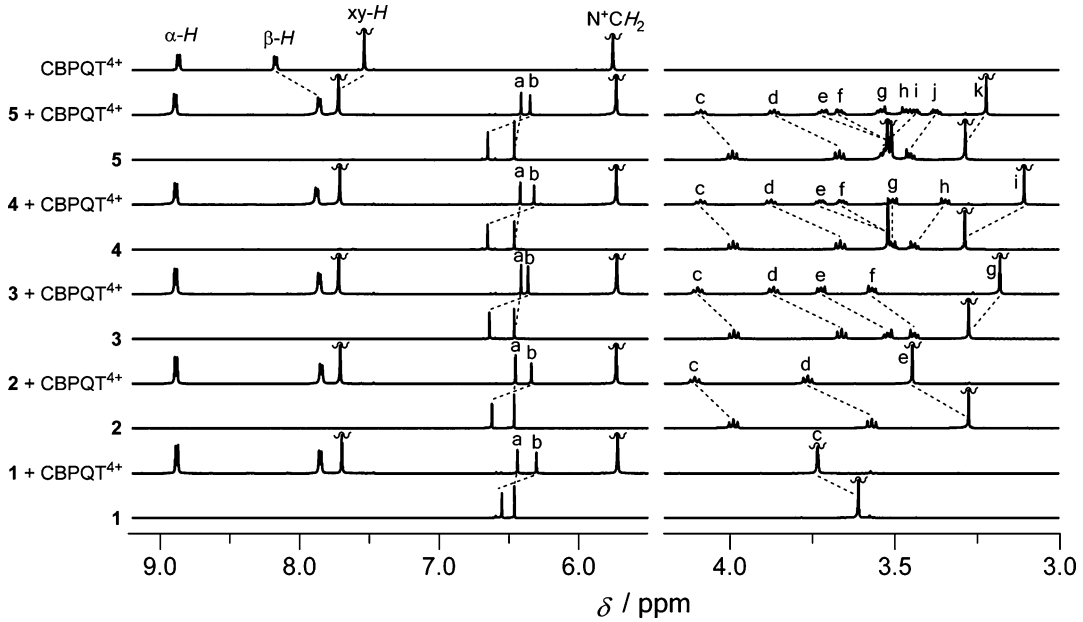

Figure 2. Partial ^{1}H NMR spectra (400 MHz) recorded in CD_3CN (c = 1.5 mM) at 298 K of $CBPQT^{4+}$, the MPTTF derivatives **1**–**5**, and equilibrated solutions containing **1**–**5** mixed with equimolar amounts of $CBPQT^{4+}$.

Table 2. ^{1}H NMR Spectroscopic Data[a] (δ Values) for All Protons in $CBPQT^{4+}$, the MPTTF Derivatives 1–5, and the [2]Pseudorotaxanes[b] 1–5⊂$CBPQT^{4+}$ in CD_3CN at 298 K[c,d]

				dithiole-*H*	pyrrole-*H*									
complex	*α*-*H*	*β*-*H*	xy-*H*	a	b	N^+CH_2	c	d	e	f	g	h	i	j	k
$CBPQT^{4+}$	8.87	8.17	7.54			5.75									
1				6.46	6.55		3.61								
1 ⊂ $CBPQT^{4+}$	8.88	7.85	7.70	6.44	6.30	5.72	3.76								
2				6.46	6.62		3.99	3.57	3.28						
2 ⊂ $CBPQT^{4+}$	8.89	7.85	7.71	6.45	6.34	5.73	4.11	3.76	3.45						
3				6.46	6.64		3.99	3.66	3.52	3.45	3.28				
3 ⊂ $CBPQT^{4+}$	8.89	7.86	7.72	6.41	6.36	5.73	4.10	3.87	3.72	3.57	3.18				
4				6.46	6.65		3.99	3.67	3.52	3.52	3.51	3.45	3.29		
4 ⊂ $CBPQT^{4+}$	8.89	7.88	7.71	6.42	6.32	5.73	4.09	3.87	3.72	3.66	3.51	3.35	3.11		
5				6.46	6.65		3.99	3.67	3.52	3.52	3.51	3.51	3.51	3.46	3.29
5 ⊂ $CBPQT^{4+}$	8.89	7.86	7.72	6.41	6.35	5.73	4.09	3.87	3.71	3.67	3.54	3.45	3.44	3.38	3.22

[a] ^{1}H NMR spectra were recorded at 400 MHz. [b] The [2]pseudorotaxanes **1**–**5**⊂$CBPQT^{4+}$ were prepared by mixing equimolar amounts (c = 1.5 mM) of **1**–**5** and $CBPQT{\cdot}4PF_6$. [c] For more details on the labeling codes, see Scheme 2. [d] For simplicity, multiplicity for the different resonances have not been included in the Table, but can be found in Figures 2, S17, S18, or in the Experimental Section.

the complexation between the MPTTF derivatives **1**–**5** and $CBPQT^{4+}$ came from a comparison of the ^{1}H NMR spectra (400 MHz, 298 K) recorded in CD_3CN (1.5 mM) of the MPTTF derivatives **1**–**5** and equilibrated solutions containing a 1:1 mixture of the MPTTF derivatives **1**–**5** and $CBPQT^{4+}$. In all five cases, the exchange between the complexed and uncomplexed species in the equilibrated solutions occurs rapidly on the ^{1}H NMR time scale (CD_3CN, 400 MHz) at 298 K since only one set of signals are observed in the ^{1}H NMR spectra (Figures 2, S17, and S18).

The ^{1}H NMR spectra reveals significant chemical-shift differences (Table 2) for several of the resonances associated with the protons in the $CBPQT^{4+}$ ring (Scheme 2) as well as in the protons directly bound to the MPTTF unit, which undoubtedly demonstrate that $CBPQT^{4+}$ is complexed to the MPTTF derivatives **1**–**5**.[21] In particular, the resonances associated with the *β*-*H* protons are upfield shifted from δ = 8.17 ppm to δ = 7.85–7.88 ppm ($\Delta\delta$ = −0.29 to −0.32 ppm) a finding that can be ascribed to CT interactions taking place when the MPTTF unit is located inside $CBPQT^{4+}$,[22] whereas the xy-*H* protons are downfield shifted from δ = 7.54 ppm to δ = 7.70–7.72 ppm ($\Delta\delta$ = +0.16 to +0.18 ppm). In addition, the signals corresponding to the pyrrole-*H* protons (Scheme 2) are upfield shifted from δ = 6.55–6.65 ppm to δ = 6.30–6.36 ppm ($\Delta\delta$ = −0.25 to −0.33 ppm), whereas the signals related to the dithiole-*H* protons experience much smaller upfield shifts from δ = 6.46 ppm to δ = 6.41–6.45 ppm ($\Delta\delta$ = −0.01 to −0.05 ppm) upon complexation of the MPTTF derivatives **1**–**5** by $CBPQT^{4+}$. The upfield shifts of the dithiole-*H* and pyrrole-*H* protons can be accounted for by the anisotropic shielding effect that takes place when the $CBPQT^{4+}$ ring encircles the MPTTF unit. Additionally, the larger upfield shift of the pyrrole-*H* protons can most likely be explained by the fact that they can participate in edge-to-face [C–H···π] interactions with the $CBPQT^{4+}$ ring by pointing toward the faces of the *p*-xylene units of $CBPQT^{4+}$, a finding that was further corroborated by

DOI: 10.1021/acs.joc.6b02466
J. Org. Chem. 2017, 82, 1371–1379

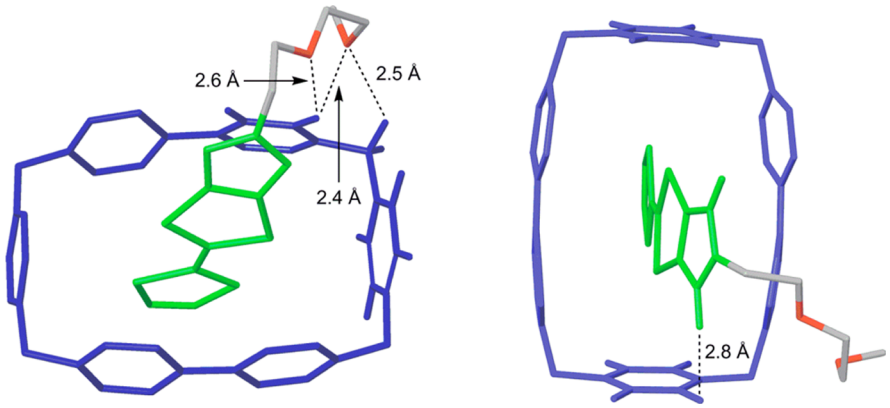

Figure 3. M06-L/6-31G** geometry optimized superstructure of the [2]pseudorotaxane **3**⊂CBPQT^{4+} (solvent corrected, MeCN) shown at two different angles. For clarity some of the hydrogen atoms have been removed; the MPTTF unit is colored green and the CBPQT^{4+} ring is blue, whereas carbon and oxygen atoms in the glycol chain are colored gray and red, respectively.

density functional theory (DFT) studies (*vide infra*). These observations also seem to indicate that CBPQT^{4+} is not positioned symmetrically around the central MPTTF double bond but instead is moved slightly toward the pyrrole ring favoring the formation of [C−H···π] interactions with CBPQT^{4+}. To provide further evidence for the existence of [C−H···π] interactions between the *p*-xylene units of CBPQT^{4+} and the pyrrole-*H* protons, a two-dimensional (2D) NOESY NMR experiment of an equilibrated solution containing a 1:1 mixture of the MPTTF derivative **3** and CBPQT^{4+} was carried out. The 2D NOESY NMR spectrum (400 MHz, CD_3CN, 298 K, 600 ms mixing time) displays (Figure S20) a clear crosspeak between the pyrrole-*H* protons of the MPTTF unit and the *p*-xylene protons of CBPQT^{4+}, which clearly show that these protons are spatially close to each other and consequently support the notion that [C−H···π] interactions between the *p*-xylene units of CBPQT^{4+} and the pyrrole-*H* protons can take place. Taken all together, these NMR spectroscopic experiments unequivocally prove that the MPTTF unit is located inside CBPQT^{4+}.

In the aliphatic region of the ^{1}H NMR spectra, it is evident that the protons closest (i.e., the c-protons, Scheme 2 and Table 2) to the MPTTF unit in **1**−**5** become downfield shifted ($\Delta\delta$ = +0.10 to +0.15 ppm) upon complexation with CBPQT^{4+}, an observation which can be ascribed to the stronger electron withdrawing inductive effect of the MPTTF unit when it is being surrounded by the CBPQT^{4+} ring as compared to the uncomplexed MPTTF unit. The resonances associated with the d- and e-protons are significantly downfield shifted ($\Delta\delta$ = +0.19 to +0.21 ppm and +0.17 to +0.20 ppm, respectively) in the [2]pseudorotaxanes **2**−**5**⊂CBPQT^{4+}. This observation can not solely be explained by the inductive effect exerted by the complexed MPTTF unit, since the inductive effect is heavily distance dependent.[23] Instead, the observed downfield shifts strongly indicate that the oxygen atoms surrounded by the d- and e-protons in **2**−**5**⊂CBPQT^{4+} are engaged in [C−H···O] hydrogen bonding interactions with the *α-H* protons in CBPQT^{4+}.[24] In the case of the [2]-pseudorotaxanes **3**−**5**⊂CBPQT^{4+}, it transpires that the resonances associated with the f-protons also are significantly downfield shifted ($\Delta\delta$ = +0.12 to +0.15 ppm) as compared to **3**−**5** demonstrating that the oxygen atom neighbor to the f-protons (i.e., the second oxygen counted from the MPPTF unit) also participate in [C−H···O] hydrogen bonding interactions with the *α-H* protons in CBPQT^{4+}. Consistent with these experimental observations, these [C−H···O] hydrogen bonding interactions are furthermore theoretically supported by DFT studies (*vide infra*) carried out on the [2]pseudorotaxane **3**⊂CBPQT^{4+}. A comparison (Figure 2 and Table 2) of the chemical shift differences between the g-protons in the [2]pseudorotaxanes **3**−**5**⊂CBPQT^{4+} and in **3**−**5** did not provide an unambiguous picture, e.g., in the case of **3**, the g-protons were upfield shifted ($\Delta\delta$ = −0.10 ppm). However, upon increasing the number of ethyleneoxy units from two to three and four (as in **4** and **5**), the g-protons in the [2]pseudorotaxanes **4**−**5**⊂CBPQT^{4+} were either not shifted (as in **4**) or slightly downfield shifted ($\Delta\delta$ = +0.03 ppm) as in **5**. These diverging observations can most likely be accounted for by the fact that the g-protons in **3** are part of a methyl group, whereas they in **4** and **5** are part of a methylene group. Moving further away from the MPTTF unit, it turns out that the signals for the h-and j-protons in **4** and the signals for the h-, j-, i-, and k-protons in **5** all experience upfield chemical shifts ($\Delta\delta$ = −0.06 to −0.13 ppm) upon complexation with CBPQT^{4+}. Because the signals for these protons are not downfield shifted, as seen for the d-, e-, and f-protons, it seems very likely that the third and fourth oxygen atoms are not being engaged in hydrogen bonding interactions with CBPQT^{4+}.

Small chemical shifts for the *α-H* protons in CBPQT^{4+} are being observed in the [2]pseudorotaxanes **2**−**5**⊂CBPQT^{4+} as compared to those of the [2]pseudorotaxane **1**⊂CBPQT^{4+}. The resonances associated with the *α-H* protons are downfield shifted from δ = 8.87 ppm to δ = 8.89 ppm ($\Delta\delta$ = +0.02 ppm) for [2]pseudorotaxanes **2**−**5**⊂CBPQT^{4+} and to δ = 8.88 ppm ($\Delta\delta$ = +0.01 ppm) for the [2]pseudorotaxane **1**⊂CBPQT^{4+} relative to CBPQT^{4+}. Since the glycol chain in the [2]-pseudorotaxanes **2**−**5**⊂CBPQT^{4+} only can form [C−H···O] hydrogen bonding interactions with one of the eight *α-H* protons present in CBPQT^{4+} at a given time, and the fact that the complexation/decomplexation process for the formation of the [2]pseudorotaxanes is fast on the ^{1}H NMR time scale, the observed chemical shifts changes will be an average for the eight *α-H* protons. Although small, the additional downfield shift observed for the *α-H* protons, when comparing the [2]pseudorotaxanes **2**−**5**⊂CBPQT^{4+} with the [2]pseudorotaxane **1**⊂CBPQT^{4+}, indicate that the *α-H* protons are engaged in [C−H···O] hydrogen bonding interactions with the glycol chains.

The 2D NOESY NMR spectrum (Figure S20) recorded on a 1:1 mixture of **3** and CBPQT^{4+} did not show any NOE effect

DOI: 10.1021/acs.joc.6b02466
J. Org. Chem. 2017, 82, 1371−1379

between the protons in the glycol chain appended to the MPTTF unit and the protons on the CBPQT^{4+} ring, which most likely can be explained by the dynamic nature of the complex and in particular of the glycol chain which is free to move on the exterior of the complex.[17] In addition, the calculated superstructure (*vide infra*) of **3**⊂CBPQT^{4+} reveals that the average distances between the *α-H* protons and the d-, e-, f-, and g-protons is 4.4, 4.0, 3.5, and 4.0 Å, respectively, which under the experimental conditions is beyond the distance where an NOE effect is expected to be observable.

Molecular Modeling. With strong experimental evidence for the formation of a folded 3° superstructure involving hydrogen bonding interactions and to get a better understanding of the binding interactions present in the [2]-pseudorotaxanes, **3**⊂CBPQT^{4+} was investigated by DFT methods to obtain a quantum mechanical (QM) based description of its geometry. The QM geometry optimization reported here use the exchange-correlation functional M06-L[25] with the 6-31G** basis set as implemented in Jaguar 9.3,[26] which has previously been used to obtain precise structural and energetic descriptions of superstructures and mechanically interlocked molecules.[17,27] The optimized superstructures were evaluated based on lowest single point energy with the 6-311++G** basis set and to correct for solvation, the implicit solvent model SM8[28] was used to simulate a solution of MeCN (R_0 = 2.2 Å; ε = 37.5). In the optimized superstructure of **3**⊂CBPQT^{4+}, it is evident (Figure 3 and Figure S21) that CBPQT^{4+} encircles the MPTTF unit. Furthermore, it shows (Figure 3, left) a geometry that is stabilized by hydrogen bonding interactions where the two oxygen atoms in the glycol chain interacts simultaneously with one of the acidic *α-H* protons of CBPQT^{4+}. These bifurcated [C−H···O] hydrogen bonding interactions have previously been observed experimentally in the solid state for catenanes and rotaxanes incorporating CBPQT^{4+} and glycol chains.[7a,29] A close inspection of the superstructure of **3**⊂CBPQT^{4+} revealed the existence of [C−H···O] hydrogen bonding interactions (i) between one of the *α-H* protons of CBPQT^{4+} and the first oxygen atom in the glycol chain ([H···O], 2.6 Å; [C−H···O], 134°) and (ii) between the same *α-H* proton and the second oxygen atom in the glycol chain ([H···O], 2.4 Å; [C−H···O], 95°). In addition, a short distance ((H···O], 2.5 Å; [C−H···O], 126°) between one of the N^+CH_2 protons of CBPQT^{4+} and the second oxygen atom in the glycol chain is also noted.

These findings are in complete agreement with our experimental studies (*vide supra*) and previously reported QM-based calculations and analyses of X-ray crystal structures carried out on similar superstructures and mechanically interlocked molecules incorporating TTF/MPTTF and CBPQT^{4+}.[7b,17,24,30]

Consistently, with the results (*vide supra*) obtained from the 2D NOESY experiment carried out on the [2]pseudorotaxane **3**⊂CBPQT^{4+}, the energy-optimized superstructure of **3**⊂CBPQT^{4+} show (Figure 3, right) that the shortest distance [H···H] between one of the pyrrole-*H* protons and one of the protons in the *p*-xylene units of CBPQT^{4+} is 2.8 Å. These observations display that the pyrrole-*H* protons are located in close distance to the *π*-cloud of the aromatic *p*-xylene units of CBPQT^{4+} allowing [C−H···*π*] interactions between the pyrrole-*H* protons and the aromatic *p*-xylene units of CBPQT^{4+} to take place.

Overall the QM calculated superstructure suggest that the geometry of **3**⊂CBPQT^{4+} is stabilized by a combination of CT, [C−H···*π*], and [C−H···O] interactions.

Binding Studies between the MPTTF Derivatives 1−5 and CBPQT^{4+}. To quantify the effect of changing the length of the glycol chains, binding studies between the MPTTF derivatives **1**−**5** and CBPQT^{4+} were carried out. Mixing the MPTTF derivatives **1**−**5** with equimolar amounts of CBPQT^{4+} in MeCN (298 K) leads (*vide supra*) to the formation of the [2]pseudorotaxanes **1**−**5**⊂CBPQT^{4+}. The UV−vis−NIR dilution method[11b] was used to determine (Figure 4) the binding

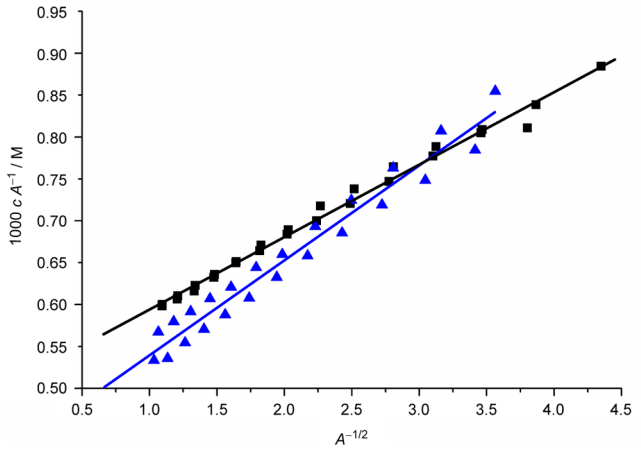

Figure 4. Linear plots of 1000 $c\,A^{-1}$ against $A^{-1/2}$ for a 1:1 mixture of CBPQT^{4+} and MPTTF derivative **1** (blue line) and **3** (black line). The absorbance A was measured at different concentrations c of CBPQT^{4+} in the range 10^{-5} − 10^{-4} M obtained from dilution of two independent stock solutions. The obtained data points [$A^{-1/2}$, $c\,A^{-1}$] were fitted to the best straight lines, giving correlation coefficients of 0.960 and 0.991, respectively.

constants (K_a) associated with the complexation using the MPTTF/CBPQT^{4+} CT band at the absorption maximum (λ_{max}) as probe. The absorbances (A) were measured at several different concentrations (c) in the range from 10^{-5} to 10^{-4} M (the exact concentrations can be found in Supporting Information) of 1:1 mixtures of CBPQT^{4+} and the MPTTF derivatives **1**−**5**. In all five cases, two independent series of measurements were made. Plotting c/A against $1/A^{1/2}$ afforded a straight line with a slope $\alpha = (1/K_a\epsilon l)^{1/2}$ and an intercept $y_0 = 1/\epsilon l$, where ϵ is the molar extinction coefficient for the CT band of the [2]pseudorotaxane in question and l is the optical path length, according to eq 1. Combining α and y_0 yields $K_a = y_0/\alpha^2$. Representative linear plots of c/A against $1/A^{1/2}$ are shown in Figure 4 for the complexation between CBPQT^{4+} and the MPTTF derivatives **1** and **3**, respectively.

$$\frac{c}{A} = \left(\frac{1}{K_a \epsilon l}\right)^{1/2} \times \frac{1}{A^{1/2}} + \frac{1}{\epsilon l} \qquad (1)$$

The K_a values obtained from these five dilution experiments were used to calculate the change in Gibbs free energy ($\Delta G°$) for the complexation process in MeCN at 298 K and are summarized in Table 3 together with λ_{max} values, the number of data points, and the correlation coefficients.

The data summarized in Table 3 reveal several significant trends. First of all, they support the finding that glycol chains can assist the complexation process between MPTTF[13]

DOI: 10.1021/acs.joc.6b02466
J. Org. Chem. 2017, 82, 1371−1379

Table 3. Binding Constants (K_a Values) and Derived Free Energies of Complexation ($\Delta G°$) between the MPTTF Derivatives 1−5 and CBPQT^{4+} Determined by UV−vis−NIR Absorption Spectroscopy at 298 K in MeCN[a]

compound	λ_{max} (nm)	data points	correlation coefficient	K_a[a,b] (M^{-1})	$\Delta G°$[b] (kcal mol^{-1})
1	877	24	0.960	33000 ± 4000	−6.2 ± 0.1
2	854	28	0.987	41000 ± 4000	−6.3 ± 0.1
3	854	27	0.991	68000 ± 8000	−6.6 ± 0.1
4	856	28	0.986	64000 ± 8000	−6.6 ± 0.1
5	854	29	0.999	63000 ± 7000	−6.6 ± 0.1

[a]The K_a values reported are for the tetrakis(hexafluorophosphate) ($4PF_6^-$) salt of CBPQT^{4+} and were obtained using the MPTTF/CBPQT^{4+} CT band at λ_{max} as probes. [b]The errors on K_a and $\Delta G°$ were obtained using the method described by Nygaard et al.[13] with ΔT = 1 K, Δc = 1%, and ΔA = 0.5%. The data in Table 3 are calculated from the slope and intersection of the linear plots shown in Figure 4 and Supporting Information.

derivatives and CBPQT^{4+}. For instance, the CBPQT^{4+} binding affinity of **4** (K_a = 64 000 M^{-1}) is approximately two times higher than that of **1** (K_a = 33000 M^{-1}). More importantly, the results unambiguously demonstrate that the length of the glycol chains has a significant impact on the binding strength between MPTTF derivatives and CBPQT^{4+}. Replacing the methyl group of the MPTTF derivative **1** (K_a = 33000 M^{-1}) with one ethyleneoxy unit (as in **2**) led to a modest increase in the binding affinity (K_a = 41000 M^{-1}) toward CBPQT^{4+}. However, by increasing the number of ethyleneoxy units from one to two (as in **3**), a significant increase in the K_a value (68000 M^{-1}) was observed. Extending the glycol chain further, as in **4** or **5**, did not increase the binding affinity toward CBPQT^{4+} when the errors are taken into account. These findings are in perfect agreement with the results obtained from the ^{1}H NMR spectroscopic investigations (*vide supra*) of the [2]-pseudorotaxanes **1**−**5**⊂CBPQT^{4+}. Consequently, it is evident that the first and especially the second oxygen atoms have a strong impact on the complexation taking place between *N*-glycol substituted MPTTF derivatives and CBPQT^{4+}, whereas extending the length of the glycol chain further does not provide additional stability to the [2]pseudorotaxane.

CONCLUSION

In conclusion, a homologous series of *N*-glycol substituted MPTTF derivatives **1**−**5** with similar donor strengths that only differ in the length of the glycol chain were synthesized. The MPTTF derivatives **1**−**5** were used to assemble the [2]-pseudorotaxanes **1**−**5**⊂CBPQT^{4+} by mixing them with the electron accepting CBPQT^{4+} ring. Absorption and ^{1}H NMR spectroscopic investigations as well as DFT calculations of the [2]pseudorotaxanes **1**−**5**⊂CBPQT^{4+} confirmed that the MPTTF donor unit was encircled by the CBPQT^{4+} ring. The [C−H···O] hydrogen bonding interactions reported to be present in rotaxanes and catenanes incorporating CBPQT^{4+} were seen here by chemical shift changes. Especially for the protons in the ethyleneoxy units which became significantly upfield shifted when the CBPQT^{4+} ring encircles the MPTTF unit. These observations indicate that the first and second oxygen atoms in the [2]pseudorotaxanes **2**−**5**⊂CBPQT^{4+}, are engaged in [C−H···O] hydrogen bonding interactions with the *α-H* protons in CBPQT^{4+}, whereas the third and fourth oxygen atoms are not. This was further supported by a computer generated superstructure of the [2]pseudorotaxane **3**⊂CBPQT^{4+}. By absorption spectroscopic investigations of [2]pseudorotaxanes **1**−**5**⊂CBPQT^{4+}, it has been possible to quantify the [C−H···O] hydrogen bonding interactions. The binding studies carried out between the MPTTF derivatives **1**−**5** and CBPQT^{4+} revealed that the complexation ability of CBPQT^{4+} with the MPTTF derivative **3** was 0.3 ± 0.1 kcal mol^{-1} higher as compared to the MPTTF derivative **1**. Increasing the length of the glycol chain further, as in **4** and **5**, did not increase the binding to CBPQT^{4+} when the errors are taken into account. The results obtained are fully consistent with the presence of hydrogen bonding interactions between the glycol chains and CBPQT^{4+} and support the notion that only the first and second oxygen provide extra thermodynamic stability to the [2]pseudorotaxanes. While small, the increase in binding affinity is not unimportant. Assuming that the relative distribution between the secondary (2°) and the tertiary (3°) superstructures is related to this free energy difference, it can be calculated[31] that the equilibrium constant (K_{eq}) between the unfolded 2° superstructure and the folded 3° superstructure is 1.7 ± 0.3. This K_{eq} value implies that approximately 63% of **3**⊂CBPQT^{4+} exists (Figure 5) in the folded 3° superstructure

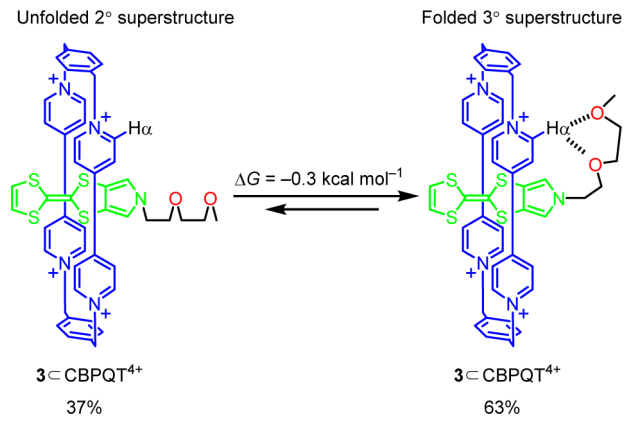

Figure 5. Equilibrium between the 2° and 3° superstructures of **3**⊂CBPQT^{4+} is shifted toward the folded 3° superstructure because an additional stabilizing effect of 0.3 kcal mol^{-1} from [C−H···O] hydrogen bonding interactions can take place on the exterior of the [2]pseudorotaxane.

in MeCN at 298 K. Overall, these insights are not unimportant and should be used as a guiding tool when it comes to future design of molecular machines based on donor−acceptor rotaxanes and catenanes.

EXPERIMENTAL SECTION

General Procedure. All reactions were carried out under an atmosphere of anhydrous N_2, unless otherwise stated. MeOH was distilled from Mg, while THF was distilled from molecular sieves (4 Å) immediately prior to use. DMF was allowed to stand over molecular sieves (4 Å) for at least 3 days prior to use. All used reagents were standard grade and used as received, except the MPTTF derivative **6**,[13] CBPQT·$4PF_6$,[7b] and the glycol-chains **8**,[18d] **9**,[18b] **10**,[18a] and **11**,[18c] which were all made according to literature procedure. Melting points (mp) were determined on a melting point apparatus and are

DOI: 10.1021/acs.joc.6b02466
J. Org. Chem. 2017, 82, 1371−1379

uncorrected. ^{1}H and ^{13}C NMR spectra were recorded at room temperature on a spectrometer at 400 and 100 MHz, respectively. Chemical shifts are quoted on the δ scale and coupling constants (J) are expressed in Hertz (Hz). Samples for ^{1}H and ^{13}C NMR spectroscopic studies were prepared using solvents in the purity they were purchased. All spectra were referenced using the residual solvent peak. The full assignment of the ^{1}H NMR signals was performed using COSY (correlation spectroscopy). Electrospray ionization (ESI) mass spectra were obtained on a mass spectrometer. Ultraviolet−visible−near-infrared (UV−vis-NIR) measurements were carried out on a UV−vis−NIR spectrophotometer in MeCN at 298 K. IR spectra were made by either making 1 mg of solid (**1** and **2**) together with 350 mg of KBr to a pellet or by putting oil (**3** **4**, and **5**) on a NaCl-film.

*2-(1,3-Dithiol-2-ylidene)-5-methyl-[1,3]dithiolo[4,5-c]pyrrole (**1**).* A solution of **6** (0.13 g, 0.55 mmol) in anhydrous DMF (20 mL) was degassed (N_2, 20 min) before NaH (55% suspension in mineral oil, 0.056 g, 2.3 mmol) and iodomethane (**7**) (0.70 g, 4.9 mmol) were added. The reaction mixture was stirred for 1.5 h at room temperature, whereupon it was degassed with N_2 for 20 min. The solvent was removed in vacuo and the residue was dissolved in CH_2Cl_2 (100 mL). This mixture was washed with H_2O (3 × 50 mL) and dried ($MgSO_4$) before the solvent was removed in vacuo. The resulting solid residue was purified by column chromatography (deactivated silica gel: CH_2Cl_2/petroleum ether (bp 60−80 °C) 1:1). The broad yellow band was collected and concentrated to provide the title compound **1** as orange crystals containing traces of grease (0.12 g, 82%): mp 155.5−160 °C; ^{1}H NMR (CD_3CN, 400 MHz) δ 3.61 (s, 3H), 6.46 (s, 2H), 6.55 (s, 2H); ^{13}C NMR (CD_3CN, 100 MHz) δ 37.6, 114.4, 115.1, 116.2, 119.1, 120.1; MS (ESI) m/z 259 (M^+ + 2), 258 (M^+ + 1), 257 (M^+); MS (HiRes−FT−ESI) Calcd for $C_9H_7NS_4^+$ 256.9456; Found 256.9455; IR ν = 3076, 2923, 1635, 1464, 1368, 1316 cm^{-1}. Anal. Calcd for $C_9H_7NS_4$ + $-CH_2-$: C, 44.25; H, 3.34; N, 5.16; S, 47.25. Found: C, 44.48; H, 3.29; N, 5.14; S, 47.12.

*2-(1,3-Dithiol-2-ylidene)-5-(2-methoxyethyl)-[1,3]dithiolo[4,5-c]-pyrrole (**2**).* A solution of **6** (0.097 g, 0.40 mmol) in anhydrous DMF (20 mL) was degassed (N_2, 15 min) before NaH (55% suspension in mineral oil, 0.087 g, 3.6 mmol) and 2-methoxy-4-methylbenzenesulfonate (**8**) (0.13 g, 0.56 mmol) were added to the yellow solution. The resulting dark orange reaction mixture was stirred for 20 h at room temperature, whereupon it was quenched by addition of H_2O (10 mL). The reaction mixture was concentrated in vacuo. The residue was dissolved in CH_2Cl_2 (125 mL) and washed with brine (50 mL) and H_2O (2 × 50 mL). The organic phase was dried ($MgSO_4$) before the solvent was removed in vacuo. The solid residue was purified by column chromatography (deactivated silica gel: 1. CH_2Cl_2, 2. CH_2Cl_2/cyclohexane 1:1) and the broad yellow band was collected and concentrated to give the title compound **2** as orange crystals containing traces of grease (0.11 g, 93%): mp 99.8−102 °C; ^{1}H NMR (CD_3CN, 400 MHz) δ 3.28 (s, 3H), 3.57 (t, 2H, J = 5.2 Hz), 3.99 (t, 2H, J = 5.2 Hz), 6.46 (s, 2H); 6.62 (s, 2H); ^{13}C NMR (CD_3CN, 100 MHz) δ 51.1, 58.9, 73.0, 114.4, 114.6, 116.1, 119.2, 120.1; MS (ESI) m/z 303 (M^+ + 2), 302 (M^+ + 1), 301 (M^+); MS (HiRes−FT−ESI) Calcd for $C_{11}H_{11}NOS_4^+$ 300.9718; Found 300.9713; IR ν = 3064, 2924, 1455, 1370, 1310, 1118 cm^{-1}. Anal. Calcd for $C_{11}H_{11}NOS_4$ + 0.4 $-CH_2-$: C, 45.09; H, 4.00; N, 4.51; S, 41.26. Found: C, 44.74; H, 3.92; N, 4.57; S, 41.09.

*2-(1,3-Dithiol-2-ylidene)-5-(2-(2-methoxyethoxy)ethyl)-[1,3]-dithiolo[4,5-c]pyrrole (**3**).* A solution of **6** (0.087 g, 0.36 mmol) in anhydrous DMF (20 mL) was degassed (N_2, 15 min), whereafter NaH (55% suspension in mineral oil, 0.062 g, 2.6 mmol) and 1-iodo-2-(2-methoxyethoxy)ethane (**9**) (0.084 g, 0.36 mmol) were added. The reaction mixture was stirred for 21 h at room temperature, after which it was quenched by addition of H_2O (10 mL) before it was extracted with CH_2Cl_2 (2 × 50 mL + 25 mL). The combined organic phases were washed with brine (2 × 50 mL) and H_2O (2 × 50 mL) before being dried ($MgSO_4$). Subsequently, the solvent was removed in vacuo and the oil residue was purified by column chromatography (deactivated silica gel: CH_2Cl_2). The broad yellow band was collected and concentrated affording the title compound **3** as a dark yellow oil (0.12 g, 97%): ^{1}H NMR (CD_3CN, 400 MHz) δ 3.28 (s, 3H), 3.43−3.45 (m, 2H), 3.51−3.53 (m, 2H), 3.66 (t, 2H, J = 5.2 Hz), 3.99 (t, 2H, J = 5.2 Hz), 6.46 (s, 2H); 6.64 (s, 2H); ^{13}C NMR (CD_3CN, 100 MHz) δ 51.2, 58.9, 71.0, 71.5, 72.5, 114.4, 114.6, 116.1, 119.2, 120.1; MS (ESI) m/z 347 (M^+ + 2), 346 (M^+ + 1), 345 (M^+); MS (HiRes−FT−ESI) Calcd for $C_{13}H_{15}NO_2S_4^+$ 344.9980; Found 344.9973; IR ν = 3064, 2873, 1453, 1369, 1308, 1134 cm^{-1}. Anal. Calcd for $C_{13}H_{15}NO_2S_4$: C, 45.19; H, 4.38; N, 4.05; S, 37.12. Found: C, 45.46; H, 4.35; N, 4.12; S, 37.24.

*2-(1,3-Dithiol-2-ylidene)-5-(2-(2-(2-methoxyethoxy)ethoxy)-ethyl)-[1,3]dithiolo[4,5-c]pyrrole (**4**).* A solution of **6** (0.073 g, 0.30 mmol) in anhydrous DMF (20 mL) was degassed (N_2, 15 min) before NaH (55% suspension in mineral oil, 0.11 g, 4.5 mmol) and 1-iodo-2-(2-(2-methoxyethoxy)ethoxy)ethane (**10**) (0.083 g, 0.34 mmol) were added. The reaction mixture was stirred for 20 h at room temperature, after which it was quenched by addition of H_2O (10 mL) and then extracted with CH_2Cl_2 (2 × 50 mL + 25 mL). The combined organic phases were washed with brine (2 × 50 mL) and H_2O (2 × 50 mL), and dried ($MgSO_4$) before it was concentrated in vacuo. The resulting oil residue was purified by column chromatography (deactivated silica gel: EtOAc) and the broad yellow band was collected and concentrated to give the title compound **4** as a dark yellow oil containing traces of grease (0.10 g, 87%): ^{1}H NMR (CD_3CN, 400 MHz) δ 3.29 (s, 3H), 3.44−3.45 (m, 2H), 3.50−3.51 (m, 2H), 3.52 (s, 4H), 3.67 (t, 2H, J = 5.1 Hz), 3.99 (t, 2H, J = 5.1 Hz), 6.46 (s, 2H); 6.65 (s, 2H); ^{13}C NMR (CD_3CN, 100 MHz) δ 51.2, 58.9, 71.0, 71.1, 71.2, 71.5, 72.7, 114.5, 114.6, 116.2, 119.1, 120.1; MS (ESI) m/z 391 (M^+ + 2), 390 (M^+ + 1), 389 (M^+); MS (HiRes−FT−ESI) Calcd for $C_{15}H_{19}NO_3S_4^+$ 389.0242; Found 389.0246; IR ν = 3066, 2915, 1452, 1369, 1307, 1103 cm^{-1}. Anal. Calcd for $C_{15}H_{19}NO_3S_4$ + $-CH_2-$: C, 47.62; H, 5.24; N, 3.47; S, 31.77. Found: C, 47.87; H, 5.22; N, 3.46; S, 31.38.

*2-(1,3-Dithiol-2-ylidene)-5-(2,5,8,11-tetraoxatridecan-13-yl)-[1,3]dithiolo[4,5-c]pyrrole (**5**).* A solution of **6** (0.062 g, 0.26 mmol) in anhydrous DMF (20 mL) was degassed (N_2, 15 min) before NaH (55% suspension in mineral oil, 0.096 g, 4.0 mmol) and 13-iodo-2,5,8,11-tetraoxatridecane (**11**) (0.084 g, 0.26 mmol) were added. The reaction mixture was stirred for 18 h at room temperature and then quenched by the addition of H_2O (10 mL), whereafter it was extracted with CH_2Cl_2 (2 × 50 mL + 25 mL). The combined organic phases were washed with brine (2 × 50 mL) and H_2O (2 × 50 mL), and dried ($MgSO_4$) before the solvent was removed in vacuo. The resulting residue was purified by column chromatography (deactivated silica gel: EtOAc) and the broad yellow band was collected and concentrated to afford the title compound **5** as a dark yellow oil containing traces of grease (0.094 g, 85%): ^{1}H NMR (CD_3CN, 400 MHz) δ 3.29 (s, 3H), 3.45−3.46 (m, 2H), 3.51−3.54 (m, 10H), 3.67 (t, 2H, J = 5.1 Hz), 3.99 (t, 2H, J = 5.1 Hz), 6.46 (s, 2H); 6.65 (s, 2H); ^{13}C NMR (CD_3CN, 100 MHz) δ 51.3, 58.9, 71.0 (× 2), 71.2, 71.2, 71.2, 71.5, 72.6, 114.5, 114.6, 116.2, 119.1, 120.1; MS (ESI) m/z 435 (M^+ + 2), 434 (M^+ + 1), 435 (M^+); MS (HiRes−FT−ESI) Calcd for $C_{17}H_{23}NO_4S_4^+$ 433.0504; Found 433.0487; IR ν = 3066, 2873, 1452, 1369, 1307, 1110 cm^{-1}. Anal. Calcd for $C_{17}H_{23}NO_4S_4$ + 1.5 $-CH_2-$: C, 48.87; H, 5.76; N, 3.08; S, 28.21. Found: C, 48.59; H, 5.76; N, 3.18; S, 27.85.

Photophysical Experiments. All experiments were carried out in air-equilibrated MeCN (HPLC grade) solutions, and hexafluorophosphate (PF_6^-) ions were the counterions in the case of all cationic CBPQT^{4+} complexes. Absorption spectra were recorded on a UV−vis−NIR spectrometer and the temperature was controlled using an electronic thermostat. The estimated experimental errors are ±0.5% on the absorbance (ΔA), ± 1% on the concentration (Δc), and ±1 K on the temperature (ΔT) unless otherwise stated.

Molecular Modeling. The computational study was carried out using the Maestro 10 release 2016−2 Schrödinger[32] package starting from the X-ray crystal structure of a [2]rotaxane incorporating an MPTTF unit and CBPQT^{4+}.[33] The GUI maestro was used to modify the structure into the [2]pseudorotaxane **3**⊂CBPQT^{4+} as well as removing the PF_6^- anions which would significantly complicate the subsequent calculations. Previous studies by Benitez et al.[27] have shown that reliable DFT studies of CBPQT^{4+} systems can be

DOI: 10.1021/acs.joc.6b02466
J. Org. Chem. 2017, 82, 1371−1379

conducted in the absence of the counterions. Molecular mechanics were used to sample for possible superstructures using macromodel[34] to run molecular dynamic simulations in the Merck molecular force field (MMFFs).[35] In total four dynamic simulations were carried out each sampling 1000 superstructures. Two were performed as molecular mechanics and two as stochastic mechanics, one of each with a constrain between the MPTTF unit and the bipyridinium moieties (0−10 Å) to avoid decomplexation of the [2]pseudorotaxane. In the other two, additional constrains between the second oxygen in the glycol chain and the *α-H* protons (0−4 Å) was used to ensure sampling of H-bonding. These simulations were run for 1 ns, at 300 K, with a 1 fs time step and using $CHCl_3$ as solvent. After sampling of these 4000 superstructures, Polak-Ribier conjugate gradient (PRCG) energy minimizations were run with MMFFs[35] in $CHCl_3$ and redundant superstructures were removed (maximum atom deviation cutoff 0.5 Å; root-mean-square deviation (RMSD) cutoff 0.5 Å, 100 superstructures saved). From these energy minimized superstructures, the eight lowest energy superstructures as well as seven superstructures with different aligning glycol chains (i.e., different hydrogen bonds between the glycol chain and $CBPQT^{4+}$) as well as a superstructure with no hydrogen bonding was chosen together with the free MPTTF and $CBPQT^{4+}$ for further DFT studies using Jaguar 9.3[26] and the exchange functional M06-L.[25] This exchange functional has been shown to give superior result in modulation of medium range interactions such as $\pi-\pi$ interactions between the MPTTF unit and $CBPQT^{4+}$.[17,27] The selected superstructures were geometry optimized at the M06-L/6-31G** level of theory in MeCN and single point energies were calculated subsequently at the M06-L/6-311++G** level of theory using the SM8 solvent model[28] for MeCN (R_0 = 2.2 Å; ε = 37.5).

Determination of Binding Constants (K_a Values) Using the UV−vis−NIR Dilution Method. The K_a values were determined using the UV−vis−NIR dilution method at 298 K. Mixing the yellow-orange MPTTF derivatives **1−5** with equimolar amounts of the colorless cyclophane CBPQT·$4PF_6$ in MeCN (HPLC grade) immediately produced green-colored solutions (for further details, see SOM). Appropriate dilutions of two independent stock solutions produced solutions with absolute concentrations (c) in the range of 10^{-4} to 10^{-5} M, which were placed in the thermostated cell compartment of the UV−vis−NIR spectrometer and allowed to equilibrate at 298 K before the absorbance spectra (see SOM) were recorded in the 200−1100 nm region. The absorbance (A) at the wavelength with maximum absorbance (λ_{max}) was used as the probe to calculate the K_a value. This resulted in 24, 28, 27, 28, and 29 data points [$A^{-1/2}$, c A^{-1}] for **1−5**⊂CBPQT·$4PF_6$, respectively. For each particular [2]pseudorotaxane **1−5**⊂CBPQT·$4PF_6$ c A^{-1} was plotted against $A^{-1/2}$, which afforded a straight line with slope α and interception y_0. To show the linear relationship, the correlation coefficients for each straight line was calculated, affording values of 0.960−0.999 (Table 3). The K_a values were obtained by using the relationship: $K_a = y_0/\alpha^2$, where $\alpha = (1/K_a\varepsilon l)^{1/2}$ and $y_0 = 1/\varepsilon l$ is the slope and y-intercept of the line, respectively.[11b]

Electrochemical Experiments. Cyclic voltammetric (CV) experiments were carried out in nitrogen-purged MeCN (HPLC grade) solutions in a classical three-electrode, single-compartment cell at room temperature. The electrochemical cell was connected to a computerized potentiostat controlled by a personal computer. The working electrode was a glassy carbon electrode and its surface was polished immediately prior to use. As reference electrode was used an $Ag/AgNO_3$ (0.01 M) electrode and as counter electrode was used a platinum wire. The concentration of the examined compounds was 1.0 mM with tetrabutylammonium hexafluorophosphate (0.1 M) added as supporting electrolyte. The measurements were carried out with a scan rate of 100 mV s^{-1} at room temperature. Based on repetitive measurements, absolute errors on potentials have been found to be less than ±5 mV. A CV of ferrocene was recorded both prior to and after the measurements on the MPTTF derivatives **1−5**, showing an $E_{1/2}$ value equal to +0.086 V.

■ ASSOCIATED CONTENT

Supporting Information

The Supporting Information is available free of charge on the ACS Publications website at DOI: 10.1021/acs.joc.6b02466.

^{1}H NMR, ^{13}C NMR, and 2D NOESY spectra as well as cyclic voltammograms of compounds **1−5**, together with details on the calculations of binding constants and XYZ coordinates for the DFT calculated superstructure of the [2]pseudorotaxane **3**⊂$CBPQT^{4+}$ (PDF)

XYZ-file of the [2]pseudorotaxane **3**⊂$CBPQT^{4+}$ (XYZ)

■ AUTHOR INFORMATION

Corresponding Author

*E-mail: joj@sdu.dk

ORCID

Gunnar Olsen: 0000-0003-2254-3543

Jan O. Jeppesen: 0000-0002-3088-2994

Notes

The authors declare no competing financial interest.

■ ACKNOWLEDGMENTS

This work was funded by the Villum Foundation and the Danish Natural Science Research Council (FNU, Project 11-106744).

■ REFERENCES

(1) (a) Lehn, J.-M. *Supramolecular Chemistry*, 1 ed.; Wiley-VCH: Weinheim, Germany, 1995. (b) Whitesides, G. M.; Grzybowski, B. *Science* **2002**, *295*, 2418. (c) Stoddart, J. F. *Nat. Chem.* **2009**, *1*, 14. (d) Thordarson, P. *Chem. Soc. Rev.* **2011**, *40*, 1305. (e) Dale, J.; Vermeulen, N. A.; Juríček, M.; Barnes, J. C.; Young, R. M.; Wasielewski, M. R.; Stoddart, J. F. *Acc. Chem. Res.* **2016**, *49*, 262.

(2) Sun, H.; Hunter, C. A.; Navarro, C.; Turega, S. *J. Am. Chem. Soc.* **2013**, *135*, 13129.

(3) (a) Stoddart, J. F. *Chem. Soc. Rev.* **2009**, *38*, 1802. (b) van Dongen, S. F. M.; Cantekin, S.; Elemans, J. A. A. W.; Rowan, A. E.; Nolte, R. J. M. *Chem. Soc. Rev.* **2014**, *43*, 99.

(4) (a) Li, S.; Huang, J.; Cook, T. R.; Pollock, J. B.; Kim, H.; Chi, K.-W.; Stang, P. J. *J. Am. Chem. Soc.* **2013**, *135*, 2084. (b) Venturi, M.; Credi, A. *Electrochim. Acta* **2014**, *140*, 467. (c) Van Quaethem, A.; Lussis, P.; Leigh, D. A.; Duwez, A.-S.; Fustin, C.-A. *Chem. Sci.* **2014**, *5*, 1449.

(5) (a) Lewandowski, B.; De Bo, G.; Ward, J. W.; Papmeyer, M.; Kuschel, S.; Aldegunde, M. J.; Gramlich, P. M. E.; Heckmann, D.; Goldup, S. M.; D'Souza, D. M.; Fernandes, A. E.; Leigh, D. A. *Science* **2013**, *339*, 189. (b) Saha, S.; Santra, S.; Akhuli, B.; Ghosh, P. *J. Org. Chem.* **2014**, *79*, 11170. (c) Meng, Z.; Xiang, J.-F.; Chen, C.-F. *Chem. Sci.* **2014**, *5*, 1520. (d) Beswick, J.; Blanco, V.; De Bo, G.; Leigh, D. A.; Lewandowska, U.; Lewandowski, B.; Mishiro, K. *Chem. Sci.* **2015**, *6*, 140.

(6) (a) Katz, E.; Lioubashevsky, O.; Willner, I. *J. Am. Chem. Soc.* **2004**, *126*, 15520. (b) Nygaard, S.; Liu, Y.; Stein, P. C.; Flood, A. H.; Jeppesen, J. O. *Adv. Funct. Mater.* **2007**, *17*, 751. (c) Fahrenbach, A. C.; Zhu, Z.; Cao, D.; Liu, W.-G.; Li, H.; Dey, S. K.; Basu, S.; Trabolsi, A.; Botros, Y. Y.; Goddard, W. A.; Stoddart, J. F. *J. Am. Chem. Soc.* **2012**, *134*, 16275. (d) Coskun, A.; Spruell, J. M.; Barin, G.; Dichtel, W. R.; Flood, A. H.; Botros, Y. Y.; Stoddart, J. F. *Chem. Soc. Rev.* **2012**, *41*, 4827. (e) Sun, J.; Wu, Y.; Wang, Y.; Liu, Z.; Cheng, C.; Hartlieb, K. J.; Wasielewski, M. R.; Stoddart, J. F. *J. Am. Chem. Soc.* **2015**, *137*, 13484.

(7) (a) Anelli, P. L.; Ashton, P. R.; Ballardini, R.; Balzani, V.; Delgado, M.; Gandolfi, M. T.; Goodnow, T. T.; Kaifer, A. E.; Philp, D.; Pietrazkiwicz, M.; Prodi, L.; Reddington, M. V.; Slawin, A. M. Z.; Spencer, N.; Stoddart, J. F.; Vicent, C.; Williams, D. J. *J. Am. Chem. Soc.* **1992**, *114*, 193. (b) Asakawa, M.; Dehaen, W.; L'abbé, G.; Menzer, S.; Nouwen, J.; Raymo, F. M.; Stoddart, J. F.; Williams, D. J. *J.*

DOI: 10.1021/acs.joc.6b02466
J. Org. Chem. 2017, 82, 1371−1379

Org. Chem. **1996**, *61*, 9591. (c) Devonport, W.; Blower, M. A.; Bryce, M. R.; Goldenberg, L. M. *J. Org. Chem.* **1997**, *62*, 885.
(8) (a) Cao, J.; Jiang, Y.; Zhao, J.-M.; Chen, C.-F. *Chem. Commun.* **2009**, 1987. (b) Ikeda, T.; Higuchi, M. *Langmuir* **2011**, *27*, 4184. (c) Andersen, S. S.; Jensen, M.; Sørensen, A.; Miyazaki, E.; Takimiya, K.; Laursen, B. W.; Flood, A. H.; Jeppesen, J. O. *Chem. Commun.* **2012**, *48*, 5157.
(9) Venturi, M.; Dumas, S.; Balzani, V.; Cao, J.; Stoddart, J. F. *New J. Chem.* **2004**, *28*, 1032.
(10) (a) Castro, R.; Nixon, K. R.; Evanseck, J. D.; Kaifer, A. E. *J. Org. Chem.* **1996**, *61*, 7298. (b) Gillard, R. E.; Raymo, F. M.; Stoddart, J. F. *Chem. - Eur. J.* **1997**, *3*, 1933.
(11) (a) Damgaard, D.; Nielsen, M. B.; Lau, J.; Jensen, K. B.; Zubarev, R.; Levillain, E.; Becher, J. *J. Mater. Chem.* **2000**, *10*, 2249. (b) Nielsen, M. B.; Jeppesen, J. O.; Lau, J.; Lomholt, C.; Damgaard, D.; Jacobsen, J. P.; Becher, J.; Stoddart, J. F. *J. Org. Chem.* **2001**, *66*, 3559. (c) Das, A.; Ghosh, S. *Angew. Chem., Int. Ed.* **2014**, *53*, 2038. (d) Hartlieb, K. J.; Liu, W.−G.; Fahrenbach, A. C.; Blackburn, A. K.; Frasconi, M.; Hafezi, N.; Dey, S. K.; Sarjeant, A. A.; Stern, C. L.; Goddard, W. A., III; Stoddart, J. F. *Chem. - Eur. J.* **2016**, *22*, 2736.
(12) Jeppesen, J. O.; Nygaard, S.; Vignon, S. A.; Stoddart, J. F. *Eur. J. Org. Chem.* **2005**, *2005*, 196.
(13) Nygaard, S.; Hansen, C. N.; Jeppesen, J. O. *J. Org. Chem.* **2007**, *72*, 1617.
(14) (a) Jeppesen, J. O.; Takimiya, K.; Jensen, F.; Brimert, T.; Nielsen, K.; Thorup, N.; Becher, J. *J. Org. Chem.* **2000**, *65*, 5794. (b) Jeppesen, J. O.; Becher, J. *Eur. J. Org. Chem.* **2003**, *2003*, 3245. (c) O'Driscoll, L.; Andersen, S. S.; Solano, M. V.; Bendixen, D.; Jensen, M.; Duedal, T.; Lycoops, J.; van der Pol, C.; Sørensen, R. E.; Larsen, K. R.; Myntman, K.; Henriksen, C.; Hansen, S. W.; Jeppesen, J. O. *Beilstein J. Org. Chem.* **2015**, *11*, 1112.
(15) Andersen, S. S.; Share, A. I.; Poulsen, B. L. C.; Kørner, M.; Duedal, T.; Benson, C. R.; Hansen, S. W.; Jeppesen, J. O.; Flood, A. H. *J. Am. Chem. Soc.* **2014**, *136*, 6373.
(16) From previous binding studies (see: ref 10) carried out between $CBPQT^{4+}$ and HQ derivatives carrying glycol chains with different length, it was found that parent HQ and HQ derivatives with two ethylene glycol (EG) units, two diethylene glycol (DEG) units, two triethylene glycol (TEG) units, and two tetraethylene (TTEG) glycol units had binding constants (K_a, MeCN, 298 K) of 18, 257, 2200, 2240, and 2520 M^{-1}, respectively. Consequently, it was concluded that the second and especially the third oxygen present in the glycol chains were most important for obtaining a high K_a value between a HQ derivative carrying glycol chains and $CBPQT^{4+}$. Since an MPTTF unit and a HQ unit have significant different size and shape, it cannot be expected that the results obtained for the HQ derivatives can be transferred directly onto MPTTF derivatives.
(17) Hansen, S. W.; Stein, P. C.; Sørensen, A.; Share, A. I.; Witlicki, E. H.; Kongsted, J.; Flood, A. H.; Jeppesen, J. O. *J. Am. Chem. Soc.* **2012**, *134*, 3857.
(18) (a) Marquis, D.; Desvergne, J.-P.; Bouas-Laurent, H. *J. Org. Chem.* **1995**, *60*, 7984. (b) Arnaud, A.; Belleney, J.; Boué, F.; Bouteiller, L.; Carrot, G.; Wintgens, V. *Angew. Chem., Int. Ed.* **2004**, *43*, 1718. (c) Leng, F.; Wang, X.; Jin, L.; Yin, B. *Dyes Pigm.* **2010**, *87*, 89. (d) Rainbolt, E. A.; Washington, K. E.; Biewer, M. C.; Stefan, M. C. *J. Mater. Chem. B* **2013**, *1*, 6532.
(19) (a) Jeppesen, J. O.; Becher, J.; Stoddart, J. F. *Org. Lett.* **2002**, *4*, 557. (b) Jeppesen, J. O.; Vignon, S. A.; Stoddart, J. F. *Chem. - Eur. J.* **2003**, *9*, 4611.
(20) Jeppesen, J. O.; Takimiya, K.; Jensen, F.; Becher, J. *Org. Lett.* **1999**, *1*, 1291.
(21) From the obtained (vide infra) binding constants (K_a) and the starting concentration of compounds **1**−**5** and $CBPQT^{4+}$ (1.5 mM) it is found that the MPTTF compounds **1**−**5** are 87−91% complexed, which is the same within the errors on the binding constants and the starting concentration. Therefore, the change in chemical shift values (Figure 2) between the different equilibrium solutions is due to the different binding strength between the MPTTF derivatives and $CBPQT^{4+}$ and hence not an evidence of different amounts of complex in the different solutions (**1**−**5**⊂$CBPQT^{4+}$).
(22) See for example ref 19b.
(23) (a) Peterson, P. E.; Casey, C. *Tetrahedron Lett.* **1963**, *4*, 1569. (b) Stock, L. M. *J. Chem. Educ.* **1972**, *49*, 400.
(24) The existence of [C−H···O] hydrogen bonding interactions between the *α-H* protons in $CBPQT^{4+}$ and glycol chains has previously been observed in X-ray crystal structures of pseudorotaxanes incorporating $CBPQT^{4+}$ as the ring component and HQ derivatives substituted with glycol chains as the thread component, see: Asakawa, M.; Brown, C. L.; Menzer, S.; Raymo, F. M.; Stoddart, J. F.; Williams, D. J. *J. Am. Chem. Soc.* **1997**, *119*, 2614.
(25) Zhao, Y.; Truhlar, D. G. *J. Chem. Phys.* **2006**, *125*, 194101.
(26) (a) Bochevarov, A. D.; Harder, E.; Hughes, T. F.; Greenwood, J. R.; Braden, D. A.; Philipp, D. M.; Rinaldo, D.; Halls, M. D.; Zhang, J.; Friesner, R. A. *Int. J. Quantum Chem.* **2013**, *113*, 2110. (b) *Jaguar*, version 9.3; Schrödinger, LLC: New York, NY, 2016.
(27) Benitez, D.; Tkatchouk, E.; Yoon, I.; Stoddart, J. F.; Goddard, W. A. *J. Am. Chem. Soc.* **2008**, *130*, 14928.
(28) Marenich, A. V.; Olson, R. M.; Kelly, C. P.; Cramer, C. J.; Truhlar, D. G. *J. Chem. Theory Comput.* **2007**, *3*, 2011.
(29) Raymo, F. M.; Bartberger, M. D.; Houk, K. N.; Stoddart, J. F. *J. Am. Chem. Soc.* **2001**, *123*, 9264.
(30) (a) Houk, K. N.; Menzer, S.; Newton, S. P.; Raymo, F. M.; Stoddart, J. F.; Williams, D. J. *J. Am. Chem. Soc.* **1999**, *121*, 1479. (b) Balzani, V.; Credi, A.; Mattersteig, G.; Matthews, O. A.; Raymo, F. M.; Stoddart, J. F.; Venturi, M.; White, A. J. P.; Williams, D. J. *J. Org. Chem.* **2000**, *65*, 1924. (c) Braunschweig, A. B.; Northrop, B. H.; Stoddart, J. F. *J. Mater. Chem.* **2006**, *16*, 32.
(31) The equilibrium constant K_{eq} for the equilibrium between the unfolded 2° superstructure and the folded 3° superstructure was calculated using the relationship $K_{eq} = \exp(\Delta G/RT)$, where R is the gas constant and T is the absolute temperature.
(32) *Maestro*, version 10.6.014; Schrödinger, LLC: New York, NY, 2016.
(33) Nygaard, S.; Laursen, B. W.; Flood, A. H.; Hansen, C. N.; Jeppesen, J. O.; Stoddart, J. F. *Chem. Commun.* **2006**, 144 and unpublished X-ray crystal structure of the locked [2]rotaxane **5**·$4PF_6$ described herein..
(34) *MacroModel*, version 11.3; Schrödinger, LLC: New York, NY, 2016.
(35) Halgren, T. A. *J. Comput. Chem.* **1996**, *17*, 490.

DOI: 10.1021/acs.joc.6b02466
J. Org. Chem. 2017, 82, 1371−1379